OPTIMISED MULTI-PARAMETER NLFM PULSE COMPRESSION WAVEFORM FOR LOW TIME-BANDWIDTH RADAR

Alexander C van Zyl[1], Erich A Wiehahn[2], Jacques E Cillers[3], Thomas R Niesler[1]

[1]*Department of Electrical & Electronic Engineering, Stellenbosch University, Stellenbosch, South Africa*
[2]*Department of Industrial Engineering, Stellenbosch University, Stellenbosch, South Africa*
[3]*CSIR, Pretoria, South Africa*

Keywords: RADAR, PULSE COMPRESSION, NON-LINEAR FM, BÉZIER, LOGIT

Abstract

The radar literature contains numerous examples of non-linear frequency modulated (NLFM) waveforms where the majority of the modulation functions are either implemented under the assumption that the radar can afford to have a large time-bandwidth product (TBP) or make use of mathematical operations that are difficult to parameterise. Although this allows good performance at a high TBP, these modulation functions perform poorly at a low TBP where commercial off-the-shelf (COTS), short-range and low-power software-defined radio (SDR) based radars operate. These SDR radars have limited bandwidth due to low sampling rates and performance suffers further when transmitting over short distances in scenarios where pulsed operation is required. This paper develops and compares various multi-parameter, optimisable NLFM waveforms based on parametric functions such as Bézier curves and the inverse logistic function (logit). Low order Bézier curves are found to give insight into the optimisation space, but the logit based NLFM and 8th order Bézier waveforms are shown to have the best performance. We conclude that the proposed NLFM waveform is attractive when considering radar applications using low cost SDR platforms.

1 Introduction

The pulse compression (PC) waveform chosen in a radar has a substantial effect on the radar's target detection performance. This is due to the large number of possible waveforms and the effect of each waveform on the temporal response of the PC stage in the signal processing pipeline. The resultant main lobe width (MLW) affects the range resolution and the peak sidelobe (PSL) level affects the detection of low radar cross-section (RCS) targets in the presence of high RCS targets or clutter. Both of these variables can be adjusted by modification of the transmitted waveform and/or modification of the receive PC filter. However, many of these techniques require a mismatch between the transmitted and received waveform which, in turn, causes a signal-to-noise ratio (SNR) loss relative to the theoretical maximum achievable SNR gain for a given TBP [1], [2].

Numerous PC waveforms have been developed [3]-[5], the majority of which revolve around certain assumptions and mathematical operators. It is therefore difficult to add parameters to the process due to the inflexible nature of these designs. In addition to this, if the radar violates the assumptions made in the design process it will not perform as expected. One prevalent assumption is that the radar operates in the high TBP regime, which is the case for most high performance, long-range radars. However, in short-range, pulsed applications the TBP is highly constrained, especially when making use of low cost Software Defined Radio (SDR) platforms. It is therefore necessary to develop a PC waveform that is not based on the assumption of high a TBP.

2 Baseline Pulse Compression Waveforms

In order to measure the performance of the PC waveforms, some existing candidates are chosen for comparison. Linear frequency modulation (LFM) is used as a baseline since it is the simplest form of modulation. The LFM waveform has the drawback that its sidelobe performance is poor, with the first sidelobe being 13 dB below the peak, although it has the narrowest achievable MLW. A NLFM waveform presented by Leśnik [3] is used as a second baseline and an example of a mathematically-developed NLFM waveform that performs well at a high TBP.

2.1 Linear Frequency Modulation

The LFM is given by:

$$f(t) = f_{\text{BW}} \left(\frac{t}{\tau} - 0.5 \right), \quad t \in [0, \tau], \tag{1}$$

where f_{BW} is the desired bandwidth of the signal.

2.2 Leśnik NLFM

Leśnik [3] proposes a NLFM waveform that is calculated using the Zak transform. The frequency modulation is given by:

$$f(t) = \frac{t - \frac{\tau}{2}}{\sqrt{\frac{\tau^2(f_{\text{BW}}^2+4)}{4f_{\text{BW}}^2} - \left(t - \frac{\tau}{2}\right)^2}}, \quad t \in [0, \tau], \tag{2}$$

where f_{BW} is the bandwidth of the signal.

3 Proposed Single Parameter Waveforms

In this section we propose two low complexity NLFM waveforms that are described as a function of a single parameter.

3.1 Logit

The logit is the inverse of the logistic function. It is presented in a form that allows it to be used for frequency modulation and is given by:

$$f(t) = -\frac{mf_{\text{BW}}}{2} \ln\left(\left(c_1\left(t - \frac{\tau}{2}\right) + c_2\right)^{-1} - 1\right), \quad t \in [0, \tau], \tag{3}$$

$$c_2 = \frac{1}{1 + e^{-\frac{0}{m}}} = 0.5, \tag{4}$$

$$c_1 = \frac{2}{\tau}\left(\frac{1}{1 + e^{-\frac{1}{m}}} - c_2\right), \tag{5}$$

$$m = e^{1-p}, \tag{6}$$

where p is the tuning parameter and f_{BW} is the signal bandwidth. A higher value of p corresponds to a higher non-linearity. It is scaled using Eq. 6 so that the linearity can scale linearly and a value of 0 corresponds to an LFM waveform, which makes the parameter easier to interpret.

3.2 Hyperbolic Sine

The hyperbolic sine (sinh) is also presented in a parametric form similar to Eq. 3. It is given by:

$$f(t) = \frac{mf_{\text{BW}}}{2} \sinh\left(c\left(t - \frac{\tau}{2}\right)\right), \quad t \in [0, \tau], \tag{7}$$

$$c = \frac{2}{\tau}\left(\sinh^{-1}\left(\frac{1}{m}\right)\right), \tag{8}$$

$$m = e^{1-p}, \tag{9}$$

where p is the tuning parameter, similar to Eq. 6, and f_{BW} is the signal bandwith.

3.3 Comparison of Single Parameter PC Waveforms

Fig. 2 compares the low TBP pulse compression of the four waveforms mentioned so far. This figure illustrates some problems encountered when designing pulse compression waveforms. The Leśnik waveform does not perform as well as expected, since it is evaluated here at a much lower TBP compared to that for which it was designed [3]. Although both the sinh and logit waveforms are optimised for a low PSL, it is clear that their MLW are drastically different and this effect will be investigated further in the following sections. In addition to this, these waveforms are very limited in their shapes and a more flexible waveform design methodology can yield better results.

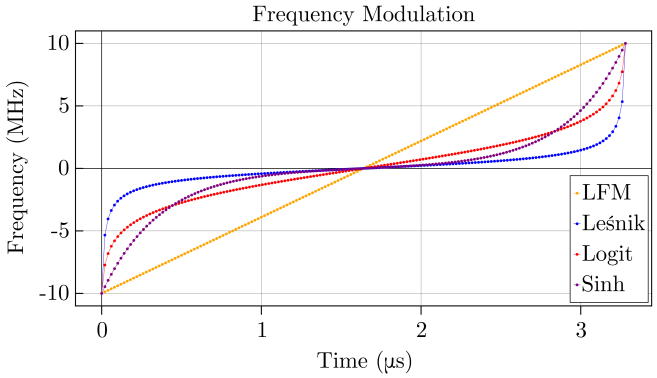

Fig. 1: The frequency modulation of the four waveforms discussed in Sec. 2 and 3.

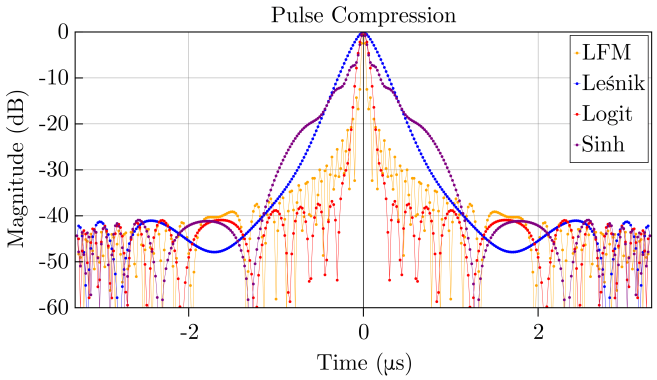

Fig. 2: A comparison of the PC of the four waveforms in Sec. 2 and 3. Both the logit and sinh are optimised for a low PSL at a TBP of 66 (bandwidth = 20MHz, transmission time = 3.33 μs and f_s = 50 MHz). The logit function parameter p is 2.282 and the sinh parameter p is 4.798.

4 Bézier Curves

Bézier curves [6] are a technique that is regularly used in computer graphics environments to define a curve using a series of vertices. It has previously been applied to radar waveform design in [7] and [8]. The number of vertices can be changed, allowing for the development of a waveform design technique with a varying number of parameters. The simplest Bézier curve has three vertices, at (0, -1), (0.5, 0) and (1, 1), giving a normalised LFM waveform. Conjugate vertices can be added to increase the complexity and non-linearity of the modulation.

The explicit form of the Bézier curve is given by

$$B(t) = \sum_{i=0}^{n} \binom{n}{i} (1-t)^{n-i} t^i P_i, \tag{10}$$

where P_i is the vertex describing the Bézier curve and n is the order of the curve, which is one less than the number of vertices. For an initial investigation, a 4^{th} order Bézier curve is used, because it allows the parameter space to be visualised in three dimensions since the x and y coordinates of only one vertex are varied. This vertex is mirrored from the positive frequency quadrant to the negative frequency quadrant to enforce symmetry in the time-frequency curve. An example can be seen in Fig. 3.

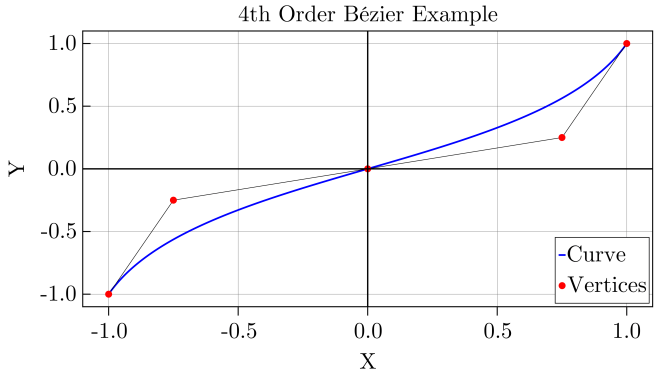

Fig. 3: An example of a waveform constructed using a 4th order Bézier curve.

Our first step was to calculate the PSL level of the waveform as the Bézier vertex position (x, y) is varied. A surface plot of these results can be seen in Fig. 4. It is highly non-linear because the sidelobe closest to the main lobe merges with the main lobe as the vertex varies, causing the PSL calculation algorithm to ignore the merged sidelobe. Instead, the next adjacent sidelobe is now regarded as the new PSL, leading to a discontinuity. It is therefore also necessary to include the zero-to-zero (0-0) MLW in the optimisation algorithm.

The 0-0 MLW plot is shown in Fig. 5 and is also highly non-linear for the same reasons mentioned for the PSL plot. To gain a better understanding of the effect of the Bézier vertex coordinate on the MLW and PSL, both plots are overlayed as a contour plot in Fig. 6.

From Fig. 6 we see there is an area in which the PSL drops drastically, but, according to Fig. 5, to reach that area the MLW must increase. Upon further investigation, it is clear that the 4^{th} order Bézier curve is not capable of generating high-performance waveforms, although the performance surface gives insight into the non-smooth characteristics of the optimisation problem. Fig. 7 shows the possible performance that a 4^{th} order Bézier curve is able to achieve with a varying vertex. We see that it is not able to surpass the performance of the optimised logit waveform. It is, therefore, necessary to investigate the performance of higher-order Bézier curves and this requires an optimisation algorithm.

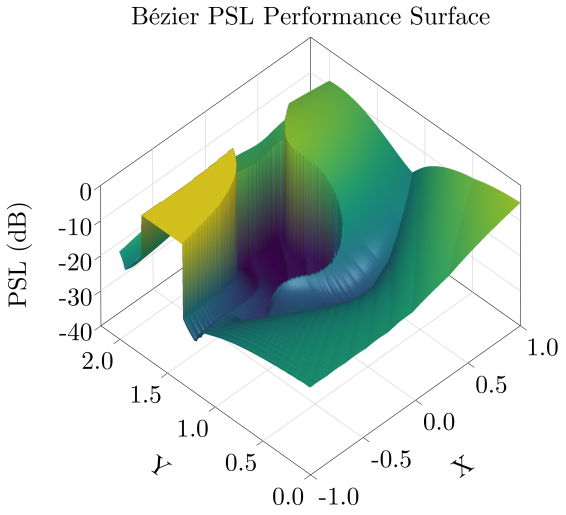

Fig. 4: The PSL of a 4^{th} order Bézier waveform where P_i in Eq. 10 is varied. The waveform has the same specifications as the waveforms in Fig. 2.

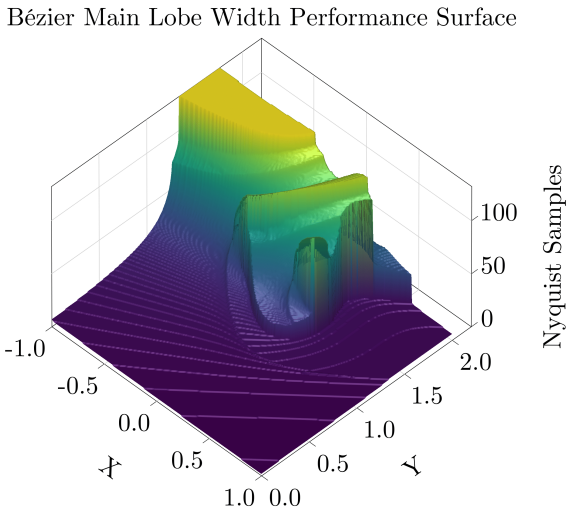

Fig. 5: The main lobe width of a 4^{th} order Bézier waveform where P_i in Eq. 10 is varied. The waveform has the same specifications as the waveforms in Fig. 2.

5 Optimisation and Results

The vertices of the Bézier curve minimising the MLW and PSL can be determined to find an optimal PC waveform. This multi-objective optimisation problem has conflicting objectives; vertices resulting in favourable values for the PSL often correspond to unfavourable values for the MLW (see Fig. 4 through 7). The fitness function given by Eq. 11 is used to combine the two objectives such that compatibility with

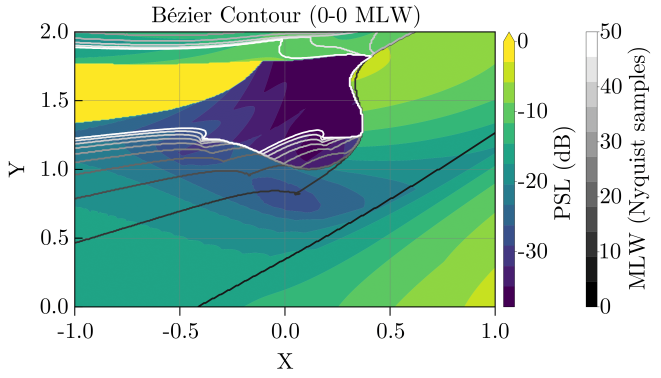

Fig. 6: The PSL (Fig. 4) and MLW (Fig. 5) plots overlayed as contour plots.

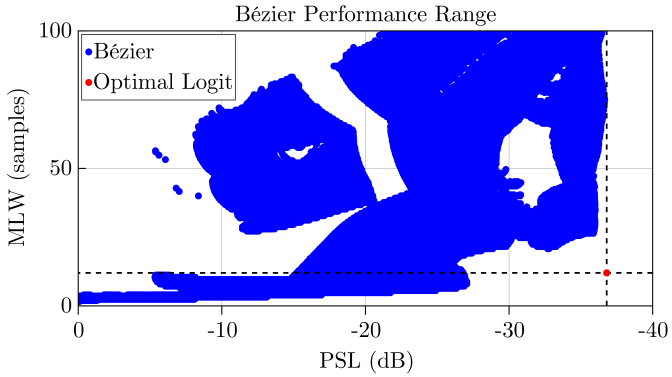

Fig. 7: The performance space (PSL and MLW), with x and y coordinates varied, for a 4^{th} order Bézier curve. The logit (optimised for PSL) is shown for reference.

single-objective optimisation methods is obtained.

$$\text{Fitness} = \alpha\text{PSL} + \frac{\beta}{\text{MLW}}, \quad \alpha \in (-\infty, 0), \quad \beta \in (0, \infty), \tag{11}$$

The aim of the optimisation algorithm is to maximise the fitness function, which simultaneously minimises the PSL and MLW. The fitness function is non-convex, non-smooth and potentially high-dimensional. Furthermore, its derivatives with respect to the vertices of the Bézier curve are not available. Gradient-based optimisation methods, such as stochastic gradient descent, are therefore not appropriate. Derivative-free optimisation methods that broadly emulate gradient descent such as the Nelder-Mead method [9] are prone to being captured by local minima and are thus not recommended for non-convex functions [10]. Brute force techniques become increasingly unfeasible for higher-order Bézier curves due to a combinatorial explosion of the problem's complexity.

Taking the aforementioned characteristics into consideration, particle swarm optimisation (PSO) [11] was chosen to maximise the fitness function. Each particle in the swarm is incentivised to explore the search space by means of an attraction factor towards the best position visited by itself while concurrently being drawn to better regions via an attraction factor towards the best global position visited by any particle in the swarm. Particles can often navigate non-convex fitness functions without becoming stuck on local maxima by retaining momentum during position updates. PSO is implemented in the Julia language [12] using Optim.jl [13] within an optimisation framework provided by Hyperopt.jl [14].

The optimiser was run for the same specifications as the waveforms in Fig. 2 and the results are presented in Fig. 8, 9 and Tab. 1. The 4^{th} order waveform performs poorly, but there is a large increase in performance when moving to the 6^{th} order waveform. Increasing the order further has little to no effect on the performance of the waveform at this TBP.

From the MLW in Tab. 1 and the spectra in Fig. 10 it can be seen that the optimisation process reduces the effective bandwidth of the waveform, thus reducing its range resolution and increasing its MLW.

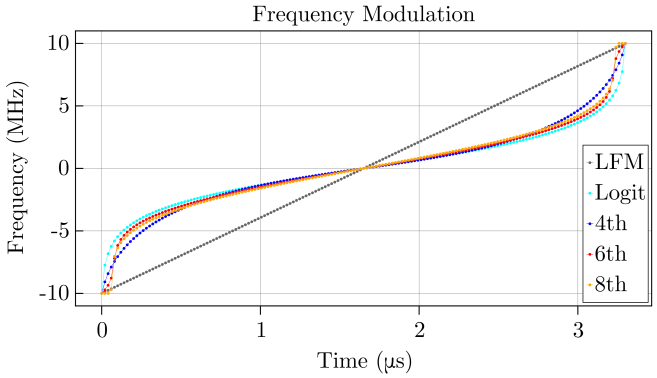

Fig. 8: A comparison of the optimal frequency modulation determined for different orders of Bézier curves. The waveforms have the same specifications as those in Fig. 2.

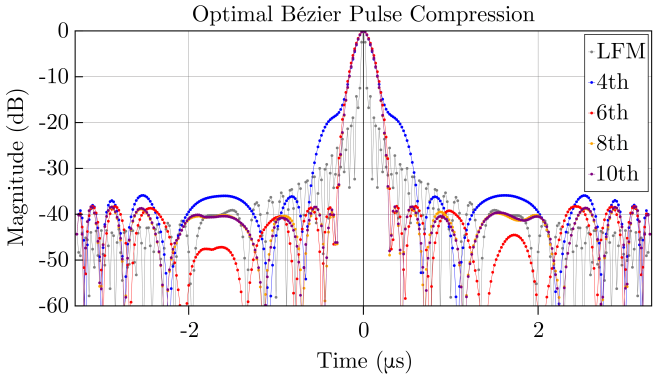

Fig. 9: Pulse compression for the waveforms shown in Fig. 8.

6 Conclusion

The aim of this paper was to develop a non-linear frequency modulated (NLFM) waveform design methodology in the low time-bandwidth product (TBP) regime that is based on parameterised functions and can thus be easily optimised. Pulse compression waveforms based on optimised Bézier curves were

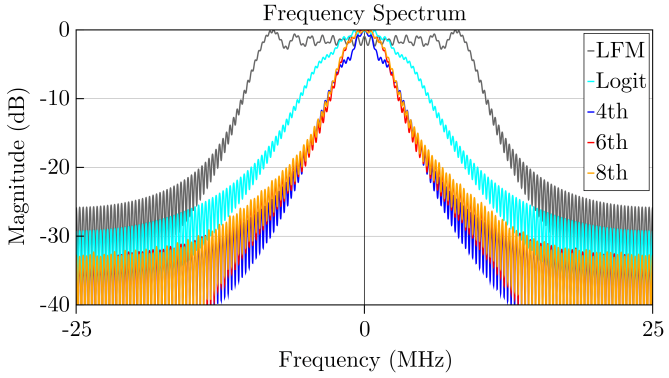

Fig. 10: The frequency spectra for the PC waveforms shown in Fig 8.

Table 1
SLL and MLW for various considered PC waveforms. All waveforms have a bandwidth of 20 MHz and transmission time of 3.33 μs. The 0-0 MLW is given when sampled at the Nyquist frequency. The different Bézier waveforms represent the various orders and different results from the optimisation algorithm.

Waveform	**PSL [dB]**	**MLW [samples]**
LFM	-14.29	2.4
Logit	-36.84	12
Sinh	-40.9	52
Leśnik	-41.1	68
Bézier (4^{th})	-35.89	26.4
Bézier (4^{th})	-27.45	6.4
Bézier (6^{th})	-38.26	12.8
Bézier (6^{th})	-37.85	12.0
Bézier (6^{th})	-36.81	9.6
Bézier (8^{th})	-38.47	12.0
Bézier (8^{th})	-38.10	11.2
Bézier (10^{th})	-38.31	12.0
Bézier (10^{th})	-38.16	11.2

found to offer improved performance over baseline methods that are effective at higher TBP.

Interestingly, the NLFM waveform based on the logit function exhibited MLW and PSL performance on par with the best Bézier based waveform for the specific TBP chosen, but this is not the case for all TBP. Thus, the logit is a better option in this case given the simplicity of implementation.

7 Future Work

In ongoing work we plan to extend the performance metrics to include the -3 dB MLW, as well as integral metrics on the sidelobe region. The current analysis should also be extended to include a spread of TBP values. Furthermore, investigations can be conducted into optimising higher-order Bézier curves and comparing the results to a variety of NLFM waveforms. This form of optimisation will also be extended to polyphase sequences and compared to results from [15] over a range of TBW values.

Due to the fact that the spectra of the NLFM waveforms are narrow compared to that of the LFM waveform, a utilised bandwidth measure, such as occupied bandwidth, can also be added to the set of metrics used by the optimisation process.

8 Acknowledgements

We thank the Council of Scientific and Industrial Research (CISR) for supporting this research.

9 References

[1] Cilliers, J.E. and Smit, J.C. : 'Pulse Compression Sidelobe Reduction by Minimization of L_p-Norms', IEEE Transactions on Aerospace and Electronic Systems, 2007, Vol. 43, No. 3, pp. 1238–1247

[2] Cilliers, J.E. and Smit, J.C. : 'On the trade-off between main lobe width and peak sidelobe level of mismatched pulse compression filters for linear chirp waveforms," 2009 European Radar Conference (EuRAD), 2009, pp. 9-12.

[3] Leśnik, C.: 'Nonlinear Frequency Modulated Signal Design', Acta Physica Polonica A, September 2009, Vol. 116, pp. 351-354.

[4] De Witte, E. and Griffiths, H.D.: 'Improved waveforms for satellite-borne precipitation radar', International Waveform Diversity & Design Conference, Orlando, United States, 2006, pp. 1-7.

[5] Doerry, A.: 'Generating precision nonlinear FM chirp waveforms', Radar Sensor Technology XI, Orlando, United States, 2007.

[6] Mortenson, M.E.: 'Mathematics for Computer Graphics Applications', Industrial Press Inc, 1999, pp. 264.

[7] Kurdzo, J., Cheong, B.L., Palmer, R. and Zhang, G.: 'Optimized NLFM Pulse Compression Waveforms for High-Sensitivity Radar Observations', IEEE Radar Conference, Lille, France, 2014.

[8] Kurdzo, J., Cho, J., Cheong, B.L. and Palmer, R.: 'A Neural Network Approach for Waveform Generation and Selection with Multi-Mission Radar', IEEE Radar Conference, Boston, United States, 2019.

[9] Nelder, J.A. and Mead, R.: 'A Simplex Method for Function Minimization', The Computer Journal, 1965, Vol. 7, Issue 4, pp. 308–313.

[10] Sparks, E.R., Talwalkar, A., Haas, D., Franklin, M.J, Jordan, M.I. and Kraska, T.: 'Automating model search for large scale machine learning', Proceedings of the Sixth ACM Symposium on Cloud Computing, New York, United States, 2015, pp. 368-380.

[11] Kennedy, J. and Eberhart, R.: 'Particle swarm optimization.', Proceedings of International Conference on Neural Networks (ICNN), Perth, Australia, 1995, Vol. 4, pp. 1942-1948.

[12] Bezanson, J., Edelman, A., Karpinski, S. and Shah, V. B.: 'Julia: A fresh approach to numerical computing', 2017,

SIAM Review, 59(1), pp. 65–98.
[13] Mogensen, P.K. and Riseth, A.N.: 'Optim: A mathematical optimization package for Julia', Journal of Open Source Software, 2018, Vol. 3, No. 24, pp. 615.
[14] Bagge Carlson, F.: 'Hyperopt.jl: Hyperparameter optimization in Julia', 2018, GitHub, https://lup.lub.lu.se/search/publication/6ec19989-9b30-448c-be5e-bae4c4257c7b.
[15] Jamil, M. and Zepernick, H. -J.: 'Sequence design for radar applications using particle swarm optimization', 2016 International Conference on Advanced Technologies for Communications (ATC), 2016, pp. 210-214.